

Article

New System to Determine the Evolution of the Dynamic Young's Modulus from Early Ages in Masonry Mortars

Engerst Yedra ¹, Daniel Ferrández ², Carlos Morón ^{1,*}  and Edmundo Gómez ¹

¹ Grupo Sensores y Actuadores, Departamento de Tecnología de la Edificación, Universidad Politécnica de Madrid, Juan de Herrera 6, 28040 Madrid, Spain; e.yedra@alumnos.upm.es (E.Y.); e.gomezl@alumnos.upm.es (E.G.)

² Grupo Sensores y Actuadores, Departamento de Organización Industrial, Administración de Empresas y Estadística, Universidad Politécnica de Madrid, Boadilla del Monte, 28660 Madrid, Spain; daniel.fvega@upm.es

* Correspondence: carlos.moron@upm.es; Tel.: +34-91-336-7583; Fax: +34-91-336-7637

Received: 26 October 2020; Accepted: 12 November 2020; Published: 17 November 2020



Featured Application: The determination of the dynamic Young's modulus by means of low-cost and non-destructive measurement techniques may represent an advance in the study of construction materials. Its application to the field of mortars made with recycled aggregates and the evolution of its mechanical properties has special relevance.

Abstract: This work presents a new method to determine the evolution of the dynamic Young's modulus (MOE) from small mechanical disturbances caused by cement mortar samples and whose value is collected using a low-cost Arduino accelerometer. The results obtained are correlated with measurements made using traditional ultrasound techniques, in addition to the evolution of MOE being related to the variation in mechanical properties that cement mortars experience over time. In this way, in this work, a secure application method is presented that allows us to advance the knowledge of construction materials with the incorporation of construction and demolition waste (CDW) and—more specifically—of cement mortars made with aggregates recycled from ceramic or concrete waste.

Keywords: dynamic Young's modulus; recycled aggregate; accelerometer; Arduino; curing process

1. Introduction

The circular economy refers to a production process in industry in which the materials that contain waste are reincorporated repeatedly for the elaboration of new products and raw materials [1]. Currently, the vast majority of generated construction and demolition waste (CDW) ends up being sent to a landfill—an action that contradicts the objectives of the 2030 horizon, where the importance of recycling and reusing all waste that can be recycled or reused is highlighted [2].

The construction sector is a prevalent consumer of raw materials. The high use of aggregates for the production of mortars and concretes stands out to the extent that approximately 85% of this material is used for this purpose [3]. However, for the aggregates to be used in the manufacture of mortars and concretes, they must have an adequate size and geometry. It is necessary to carry out crushing and separation processes for the CDW if recovery is to be efficiently achieved [4]. Various factors come into play in this process—the origin of the waste, the treatment and washing of the aggregates, the separation at source, etc.—and crucially influence the quality of the final product obtained [5–7]. Two types of recycled aggregates have been used to carry out this work: concrete and ceramic. Concrete

recycled aggregate is obtained from specific structural waste recycling processes with a low content of ceramic and bituminous particles (it is considered to be recycled concrete aggregate if it contains more than 90% of concrete) [8,9]. On the other hand, recycled ceramic aggregate has a content of ceramic material exceeding 90% and is characterized by higher absorption and a lower density [10].

A fundamental characteristic of mortars, which are known for their subsequent application on-site or their use as a restoration material, is their deformation capacity under the different stresses that may appear. It is well known that excessively rigid mortars vary the building's structural behavior as a whole and increase the risk of cracks and other constructive pathologies [11]. Thus, the determination of the Young's modulus of construction materials is essential to improving our understanding of the relationship between the stresses and deformations of the content [12]. This physical property becomes even more critical in the case of cement mortars made with recycled aggregate, as highlighted by some investigations. These have a negative influence, causing a decrease in the mechanical resistance to bending and compression, as well as more significant shrinkage during drying and lower adherence values [13,14].

Among the measurement techniques of Young's modulus in the laboratory, we find static tests employing the application of a progressive load that allows the deformation produced when the material is under particular stress to be collected, along with dynamic tests. The best-known approach is the ultrasound method, which allows the dynamic Young's modulus to be determined with the help of the propagation speed of the ultrasonic waves in the material under study [15,16]. Among the alternative techniques successfully applied in the last decades for the determination of this dynamic Young modulus in mortars, non-destructive tests consisting of the application and measurement of acoustic waves generated by the impact on the material have gained great importance [17]. In this way, Rosell, J.R. and Cantalapiedra, I.R. have adapted the test methodology included in the UNE-EN ISO 12680-1 [18] standard. To determine the dynamic Young's modulus in refractory products, tailored in lime and cement mortars, a strong correlation between the results was obtained with this method, and the measurements were collected with the aid of strain gauges [19,20]; this correlation has also been studied in buildings in Italy, in which a strong relationship between the evolution of compressive strength and dynamic Young's modulus was observed [21]. In contrast, other studies have opted for the use of measurement techniques such as infrared thermography that allow imperfections and preferential breakpoints that decrease the elastic behavior of the material to be detected [22,23]. On the other hand, other studies have shown how water saturation in mortars decreases their static and dynamic mechanical strength [24]. Finally, other authors have chosen to determine the influence of mixing water on the evolution of the resistance of mortars made with recycled aggregate, where a strong relationship was obtained between the age at which the binder material was tested and the increase of mechanical resistance [25].

Over the past decade, many research projects have emerged that use Arduino technology in their measurement equipment. Barroca et al. have used low-cost equipment to monitor humidity and temperature properties within concrete structures and collect data in real-time [26]. Some authors have used this equipment to determine material properties such as setting times using resistive sensors that vary their electrical conductivity as the material dries out [27]. Craveiro et al. show that it is possible to use automated systems with Arduino to manufacture construction elements with pre-established thermo-mechanical performances [28]. Furthermore, studies aimed at accurately monitoring and measuring the dynamic Young's modulus are especially relevant. In this sense, the work of Panda et al. [29] analyzed the mechanical properties in terms of deformation of some construction materials with the aim of extrapolating the results to large-scale printed concrete manufacturing [30].

This work aims to study the evolution of the dynamic Young's modulus in cement mortars made with recycled aggregate and its relationship with the material's physical and mechanical properties. A further aim is to validate a new measurement system to determine the speed of wave propagation through the mortar based on low-cost Arduino sensors so that these measurements can be correlated with those collected by the traditional method of ultrasound.

2. Methodology

2.1. Design and Development of a Measurement System with Arduino

The measurement equipment developed in this work allows us to measure the propagation speed of the vibrations produced by impact through the mortar specimens as the setting process evolves and therefore as its density and dynamic Young's modulus change. In this way, a reliable and low-cost system is proposed that is capable of collecting the variations produced in the response of the sensor in temporal terms for subsequent use in the calculation of the speed of propagation of vibrations through the mortar. The following devices have been used to build the measurement equipment: an Arduino Uno Rev3, as one of the platforms with the most information available and widely used in research projects [31], a 10 k Ω resistor, a push-button to initialize the taking of measurements and an Arduino-compatible MMA8451 type accelerometer. The equipment connection diagram and a simplification of the programming used are shown in Figure 1.

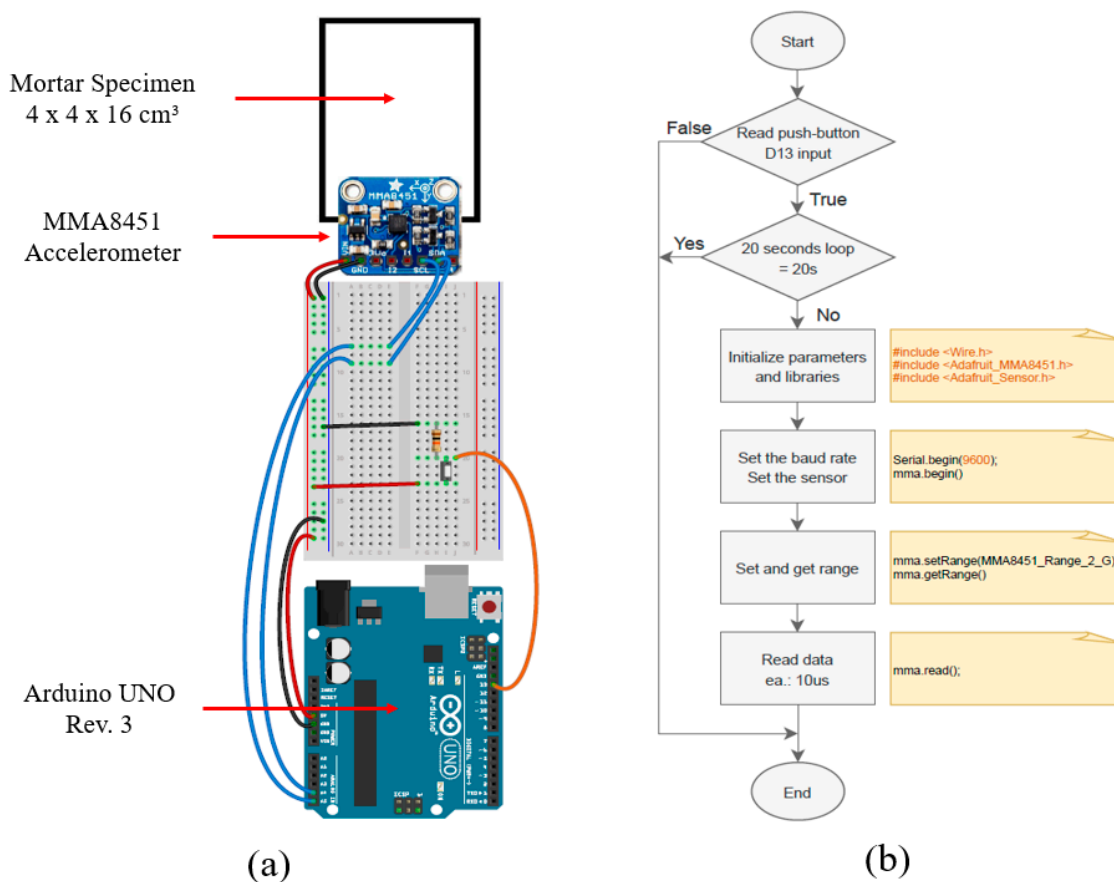


Figure 1. (a) Mounting diagram of the accelerometer used with Fritzing software; (b) simplified flow diagram of the programming carried out.

As shown in Figure 1, the Arduino board has a model ATmega328P processor, which has the following characteristics: 32 kB of flash memory, 1 kB of EEPROM (Electrically Erasable Programmable Read-Only Memory) and 2 kB of SRAM (Static Random-22Access Memory). The processor is capable of executing hundreds of thousands of instructions per second, allowing the system design to be optimized in terms of energy consumption and processing speed. This is a very significant advantage as the measurement of the rate of propagation of vibrations through the mortar involves the collection of data on the order of microseconds.

On the other hand, the MMA8451 sensor allows us, among other functionalities, to detect movement, inclination, orientation and transient responses as a digital accelerometer [32]. It is a

high-precision sensor with a 14-bit ADC (analog–digital converter) and is versatile, easy to use and compatible with Arduino and other microcontrollers.

For the calibration tests and data collection with the designed Arduino equipment, a laptop was used, with one of its USB ports used as a power source. Besides, Arduino Uno programming was carried out with the Arduino platform's program (IDE, Integrated Development Environment), where it is recommended, when starting its programming, to identify the port of the computer to which it is connected. In the program, a *.txt file was created to save the responses of the sensor collected over time, observing a peak value in the measurements when the accelerometer received an impact being produced on the mortar sample as well as the time, which were used in turn to calculate the speed of vibration propagation through the solid. Finally, it should be noted that the total sum of the components that made up the developed measurement equipment represented a total cost of around 25 €.

2.2. Experimental Program

For the determination of the dynamic Young's modulus in mortars by the traditional method, Ultrasonic Tester E46 model ultrasound measuring equipment, equipped with 55 kHz receiver–transmitter contact probes, was used. The passage time readings were created in the longitudinal direction of the standard RILEM samples with a size of $40 \times 40 \times 160 \text{ mm}^3$, as shown in Figure 2a. The speed of the ultrasonic pulse passing through the mortar sample was calculated as

$$v_{ul} = \frac{L \left[\frac{\text{m}}{\text{s}} \right]}{t} \quad (1)$$

where L is the length of the mortar specimen, which in the case of this study is 16 cm, and t is the time of passage of the ultrasonic pulse between probes, measured in seconds.

From the results obtained for the propagation speed of the ultrasound waves, it was possible to determine the modulus of the dynamic elasticity of the tested mortar samples with the help of the following equation:

$$MOE = v_{ul}^2 \times \left(\frac{\rho_n}{g} \right) \times \frac{(1 + \mu)(1 - 2\mu)}{(1 - \mu)} [\text{GPa}] \quad (2)$$

where v_{ul} is the speed of propagation of the ultrasound waves along the longitudinal dimension of the specimen in m/s, ρ_n is the density of the material on day n of the test measured in kg/m^3 , g is the acceleration of gravity in m/s^2 , and μ is the Poisson coefficient, which can be estimated to be between 0.2–0.3 for cement mortars [33,34].

On the other hand, and as an alternative method to determine the propagation speed, the Arduino equipment described and shown in Figure 2b was used. In this case, the propagation speed of the longitudinal waves produced after the impact was determined, a weight of 400 g was dropped freely on the center of one of the lateral faces of 1600 mm^2 , avoiding the displacement of the sample. An MMA8451 accelerometer was placed on the opposite face to collect the signal. Once the mechanical disturbance was transmitted in the longitudinal direction of the sample, the propagation speed was calculated as

$$v_{ac} = \frac{L}{t_1 - t_0} \left[\frac{\text{m}}{\text{s}} \right] \quad (3)$$

where t_0 is the known time that it takes for the striking equipment to contact the surface of the sample after its release, and t_1 is the time it takes for the sensor located on the opposite side to detect the vibration produced after impact.

These tests have significant relevance for construction materials placed on-site as their behavior under dynamic actions, such as experimental impacts on their surface, differs highly from their response under static actions. In general terms, these actions can cause damage to the material that abruptly compromises its structural stability; additionally, the results of these actions are more difficult to predict than deformations and stresses under static loads [35].

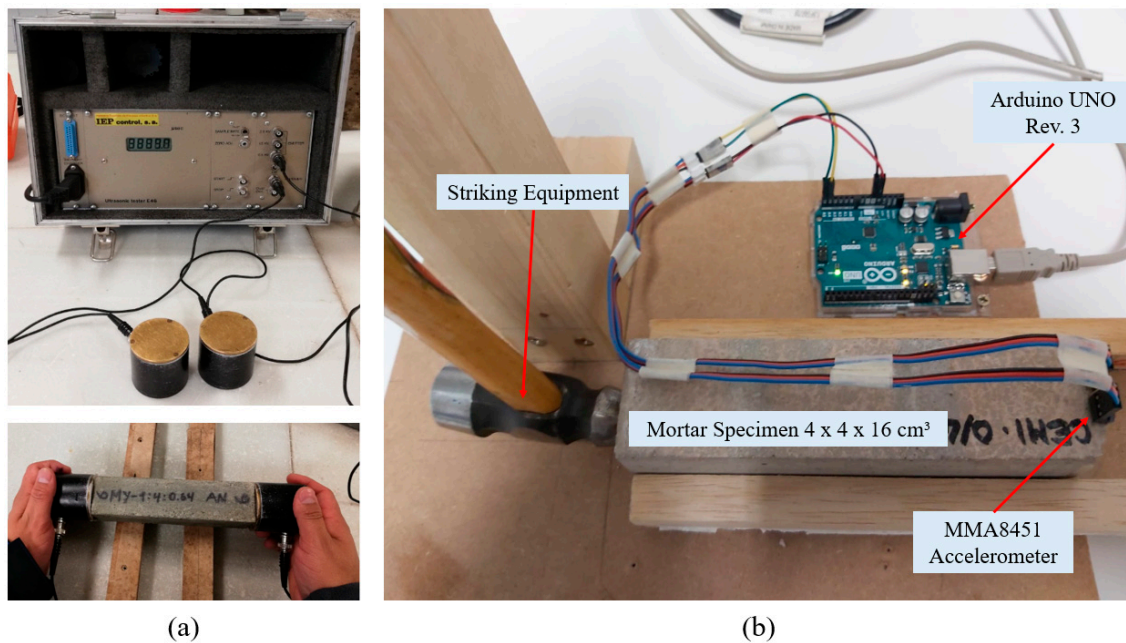


Figure 2. (a) Ultrasonic tester E46 measurement equipment and taking of measurements; (b) measurement equipment implemented in Arduino.

Lastly, the series of complementary tests collected in Table 1 were carried out to study the progression of mechanical properties in mortars made over time.

Table 1. Complementary tests for the determination of the mechanical properties in mortars.

Normative	Description
UNE-EN 1015-11:2000/A1:2007 [36]	Determination of flexural and compressive strength in mortar specimens. Measured at 7, 14, 28, 56 and 72 days.
UNE-EN 1015-12:2016 [37]	Determination of the adherence of the mortar to a previously moistened brick factory.
UNE-EN 1015-18:2003 [38]	Determination of the water absorption coefficient by the capillarity in mortars.
UNE 80-112-89 [39]	Determination of the retraction by drying in $25 \times 25 \times 287 \text{ mm}^3$ specimens by measuring changes in length.

The Shore D surface hardness test, which is not included in the test standards for cement mortars, was also carried out.

2.3. Materials and Dosages Used

The following materials were used to prepare the mortar specimens used in this study: gray cement, natural aggregate, recycled aggregate from ceramic residues, recycled aggregate from concrete wastes, water and superplasticizer additive.

2.3.1. Cement

The cement used in this work was of the type CEM II B/L-32.5 N, consisting of Portland clinker, limestone filler and up to 5% of additions [40]. This type of cement, which is commonly used in the manufacture of mortars, is regulated in RC-08 [41]. The chemical composition of the adhesive used and its thermogravimetric analysis are presented in Table 2.

Table 2. Characteristics of the type CEM II B/L-32.5 N cement used.

Chemical Composition												
Al ₂ O ₃	CaO	Fe ₂ O ₃	K ₂ O	MgO	SiO ₂	TiO ₂	MnO	P ₂ O ₅	SO ₃	BaO	SrO	Others
4.02	67.30	3.39	0.65	1.23	18.33	0.19	0.06	0.12	4.31	0.06	0.07	0.27
Thermogravimetric Analysis												
Sample	(% Total mass loss)		(% Partial mass loss)		Range of Temperatures (°C) *			Compound associated to the event				
CEM II B/L-32.5 N	8.55		0.44		<200			Gypsum				
			0.21		400–450 (441)			Ca(OH) ₂				
			7.71		450–800 (742)			Ca(CO) ₃				

* The temperature at which the maximum mass loss occurs in the event is indicated in parentheses.

The analysis in Table 2 shows that the CEM II used in this investigation is mainly composed of Al, Ca, Fe and Si oxides, according to the main phases of the Portland cement clinker. The content of sulfur oxide (SO₃) indicates the presence of gypsum in the binder material to avoid the so-called lightning setting [42]. As for the thermogravimetric analysis, it can be seen that the first loss of mass occurs in the endothermic decomposition of CaCO₃ to obtain CaO. Furthermore, two mass losses of less than 1% are shown, which are associated with the dehydration of the gypsum and the dissolution of calcium hydroxide.

2.3.2. Aggregates

The physical characterization of the aggregates used was carried out following the UNE-EN 13139: 2002 standard [43]. The results obtained are shown in Table 3.

Table 3. Physical characterization of natural aggregate (NA), recycled arid ceramic (RA-Cer) and R-recycled concrete aggregate (RA-Con).

Test	Fine Content (%)	Particle Form	Fineness Modulus (%)	Friability (%)	Bulk. Dens. (kg/m ³)	Dry Dens. (kg/m ³)	Water Absorption (%)
Standard	UNE EN 933-1 [44]	UNE-EN 13139 [43]	UNE-EN 13139 [43]	UNE-EN 146404 [45]	UNE-EN 1097-3 [46]	UNE-EN 1097-6 [47]	UNE-EN 1097-6 [47]
NA	2.45	-	4.26	21.33	1542	2503	0.96
RA-Cer	4.53	Not relevant	5.56	25.11	1254	2124	7.58
RA-Con	3.91	Not relevant	4.12	23.98	1321	2204	5.87

As shown in Table 3, the percentage of fineness in recycled aggregates is higher than that of natural aggregate, with the aggregate from ceramic waste having the highest value of this property (almost double the natural aggregate). This higher percentage of fines leads to higher water absorption and lower final mortar resistance. On the other hand, both aggregates from CDW present lower density values compared to natural aggregate, with the aggregate from ceramic waste having the lowest density.

The granulometric distribution of aggregates used for the preparation of the mortars used in this investigation was obtained according to the UNE-EN 933-2: 1996 and UNE-EN 933-1: 2012 standards [44,48]. The results are shown in Figure 3. In the case of aggregates from CDW, the fine fraction between the bottom and that retained in the 0.063 sieve was eliminated to improve the workability of the mortar. All the distribution curves of the aggregates presented are continuous and located within the limits of the regulations.

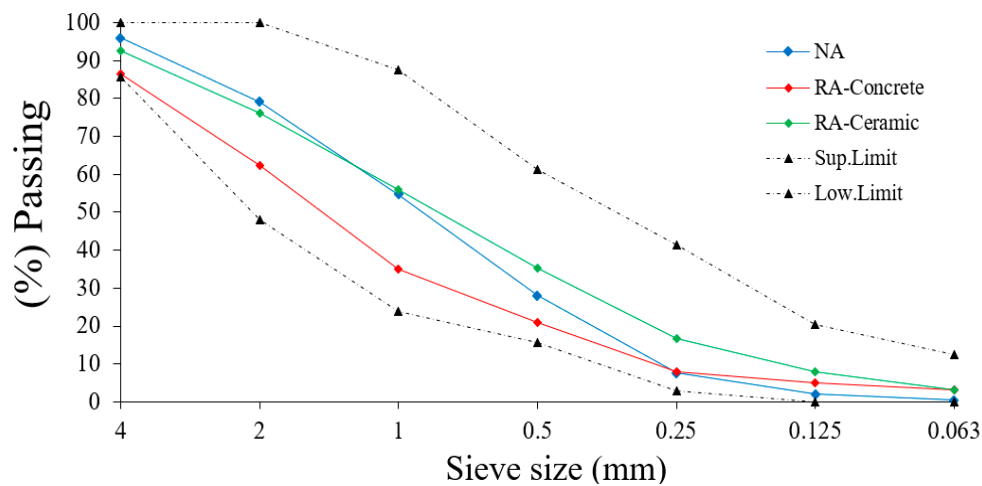


Figure 3. Recycled aggregate size distribution curve compared to the limits of NBE.FL 90 [49] adapted to the sieve size established by UNE-EN-933-2 [48].

Finally, the crystalline phases in the aggregates from construction and demolition waste used in this investigation were also identified. An X-ray diffraction test was carried out using a Siemens D5000 Diffractometer with a graphite monochromator. A Cu-K α monochromatic X-ray beam with wavelength of $\lambda = 1.540598 \text{ \AA}$ was used. In Figure 4, the results obtained can be seen at a rate of passage of the first beam every 20 s and were analyzed using the EVA software from the Bruker company, which is the characteristic of the diffractometer.

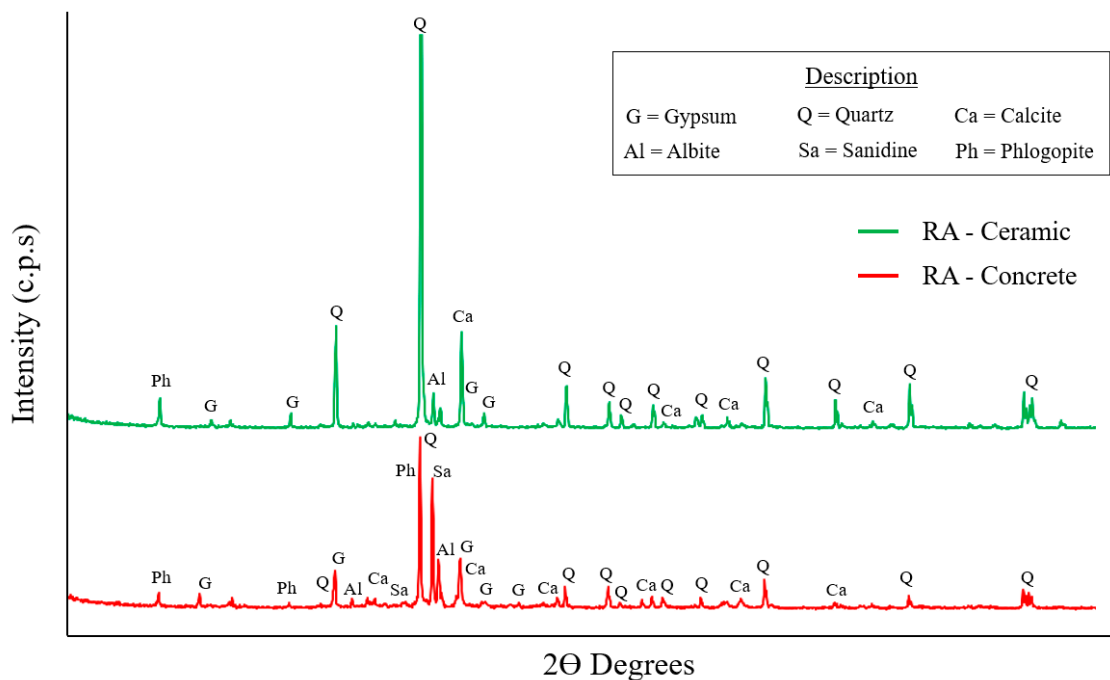


Figure 4. Diffractogram corresponding to the recycled ceramic aggregate and the recycled concrete aggregate.

The crystalline phases found in Figure 4 after the analysis of the aggregates used in this study show broad peaks and low intensities (except for quartz). This behavior is typical of compounds which have amorphous phases or a low level of crystallization, mainly caused by the components formed in the hydration of the concrete and materials that come from ceramic elements that have undergone grinding processes, as was the case for the recycled aggregates used [50].

2.3.3. Water

In this work, drinkable water from Canal de Isabel II of the Community of Madrid was used, the properties of which are shown in Table 4. The table shows that the pH remains above five, avoiding setting disturbances and excessive decreases in strength and durability, as indicated by EHE-08 [40].

Table 4. Characteristics and chemical analysis of water in the Community of Madrid [51].

Origen		Hardness		pH		Content in Cl
Low salt granite ground		Soft 25 mg CaCO ₃ /L		Min. 7	Max. 8.5	1–1.5 mg/L
Nitrates	Nitrites	Calcium	Iron	Fluorides	Sulfates	Copper
0.6 mg/L	<0.05 mg/L	17.8 mg/L	0.01 mg/L	<0.1 mg/L	5.3 mg/L	<0.005 mg/L

2.3.4. Additive

To improve the consistency of the mortar mixes made with recycled aggregate, a superplasticizer of type Glenium Sky 604 supplied by the BASF Company was used. This additive was recommended by the technical department of BASF and successfully used in other investigations [52]. It is a reliable water reducer whose raw material is formaldehyde- β -naphthalenesulfonate condensate. These types of compounds are formed by surfactant macromolecules capable of neutralizing the electrical charges of the binder grains and therefore increasing the flocculation capacity, in addition to improving workability and reducing the demand for water in fresh mortar.

2.3.5. Dosages Used

For the preparation of the mortar mixes presented in this study, the UNE-EN 196-1 standard recommendations were followed [53]. The description used in this work to name the different mortar samples adheres to the following terminology:

$$MY - A - R \quad (4)$$

where *MY* means cement mortar and *A* indicates the type of aggregate, which can be AN if it is natural aggregate, ARC if it is ceramic recycled aggregate and ARH in the case of concrete recycled aggregate. Finally, *R* represents the cement/aggregate ratio, which can be 1:3 or 1:4. Besides this, to homogenize the study and set the same mixing water content, all the test tubes prepared for each dosage came from the same mix.

The dosages used can be seen in Table 5. It should be noted that the water content in these dosages was experimentally set to achieve a plastic and workable consistency (corresponding to a diameter of the mortar paste of 175 ± 10 mm) as to the reference regulation UNE-EN 1015-2: 2007 [54].

Table 5. Dosages used to make the mortar mixes. MY: cement mortar.

Denomination	Cement/Aggregate Ratio	Water/Cement Ratio	(%) Plasticizer in Relation to the Weight of Cement
MY-NA—1:3	1:3	0.61	-
MY-NA—1:4	1:4	0.65	-
MY-RA-Cer—1:3	1:3	0.76	1
MY-RA-Cer—1:4	1:4	0.89	1
MY-RA-Con—1:3	1:3	0.73	1
MY-RA-Con—1:4	1:4	0.84	1

3. Results and Discussion

3.1. Evolution of the Dynamic Young's Modulus over Time

Figure 5 shows the variation in the longitudinal waves' propagation speed, which was generated using ultrasound impulses transmitted through the different mixes. Furthermore, since the mortars are solid materials, the positive effect of the higher density of mortars made with aggregate is noted as being natural as it has a greater top speed of propagation through the ultrasonic waves [55]. Mortars made with recycled ceramic aggregate have the lowest propagation speed values. In all cases, mixes with a cement/aggregate ratio of 1:3 had the highest propagation speeds due to their greater compactness and cement content.

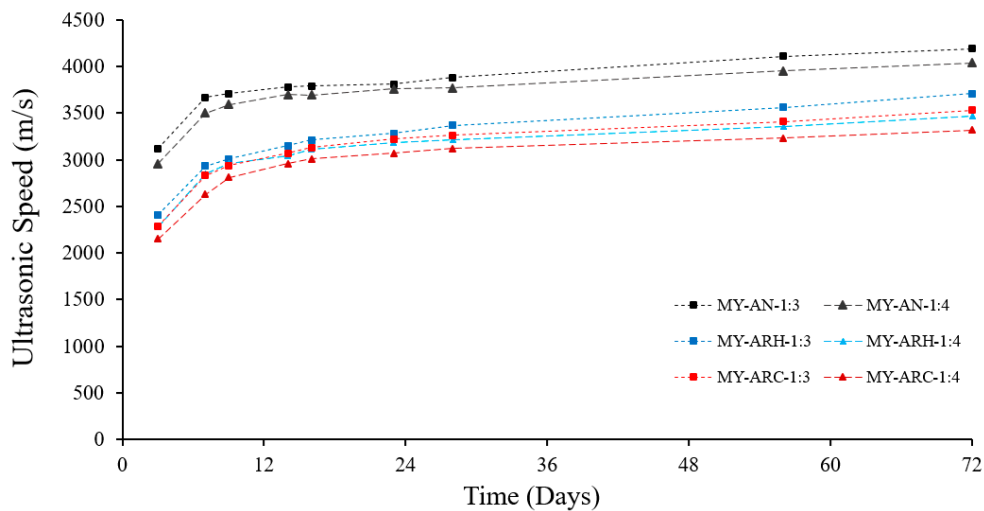


Figure 5. Variation of the propagation speed of ultrasound (m/s) versus time (days) for the prepared mortar specimens.

Figure 6 shows the evolution of the dynamic Young's modulus against time. In all of the samples analyzed, the development of this property followed a logarithmic progression, with the highest values being found in the specimens made with natural aggregate—a result that is in accordance with the values obtained in Figure 5. Ceramic presented the lowest dynamic Young's modulus values; furthermore, cement/aggregate ratio dosages of 1:4 showed lower costs than their 1:3 ratio counterparts.

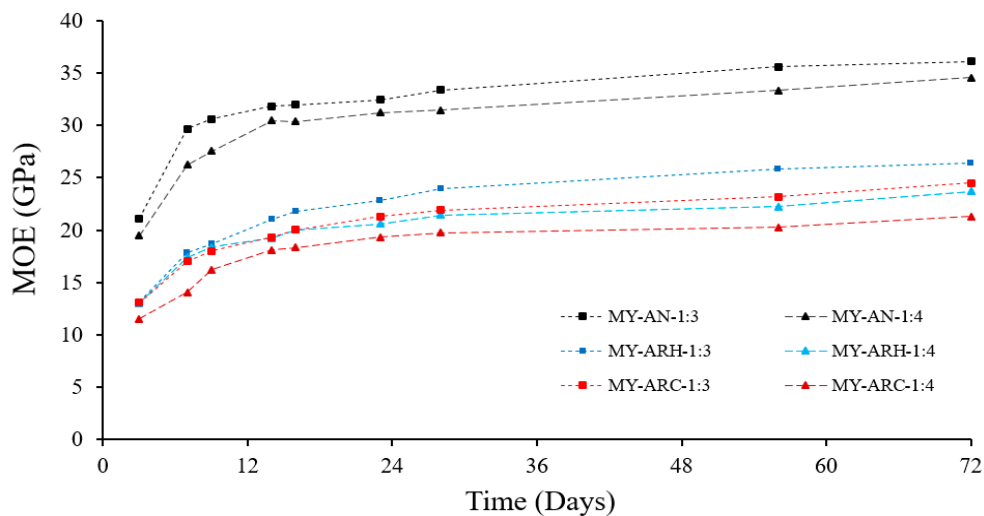


Figure 6. Evolution of the dynamic Young's modulus (MOE) (GPa) versus time (days) for the prepared mortar specimens.

3.2. Evolution of the Dynamic Young’s Modulus and Its Relationship with the Measures of the Designed Equipment

Figure 7 shows the evolution of the propagation speed of the longitudinal waves produced by impact through the mortar. These values were measured with the help of the Arduino sensor system designed for this study and in the same specimens as those in the ultrasound test.

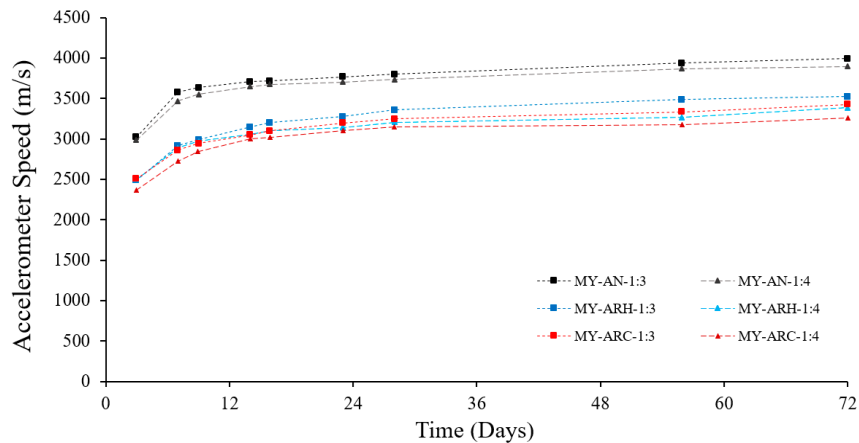


Figure 7. Evolution of the speed calculated through the time measurements collected with the Arduino equipment.

As can be seen in Figure 7, the behavior of the propagation velocity values calculated through the accelerometer measurements reflect a similar trend to the velocity measurements captured with the ultrasound equipment. On the other hand, Figure 8 presents the correlation between the measurements collected with the ultrasound method and the Arduino equipment with an accelerometer. The values of the regression lines obtained and their coefficient R^2 for each type of mortar are collected in Table 6.

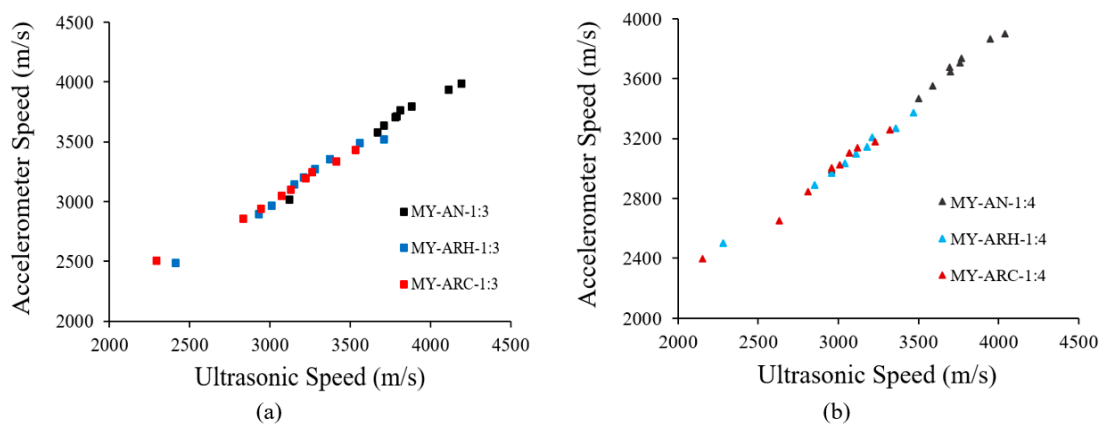


Figure 8. Correlation between the speeds measured with ultrasound and the rates measured with the Arduino equipment. (a) Mortars with a cement/aggregate ratio of 1:3; (b) mortars with a cement/aggregate ratio of 1:4.

As can be seen in Figure 8, supported by Table 6, the speeds calculated through the time measurements collected with the MMA8451 sensor and the rates taken with the ultrasound equipment follow a strong positive correlation. Thus, it is possible—with the appropriate calibration of the accelerometer—to relate both measurements to the calculation of the dynamic Young’s modulus in cement mortars. Furthermore, the ease of the execution of the test, as well as the low cost of the Arduino equipment, allow us to propose the widespread application of this measurement method

as a control tool in mortar production plants and for the characterization of this type of material in laboratory tests.

Table 6. Linear regression adjustments and R^2 coefficients for the relationship of speed measurements obtained by ultrasound and by the Arduino system.

Type	Equation	R^2	Type	Equation	R^2
MY-NA—1:3	$y = 0.9131x + 228.47$	0.9758	MY-NA—1:4	$y = 0.8710x + 426.61$	0.9925
MY-ARH—1:3	$y = 0.8515x + 441.91$	0.9836	MY-ARH—1:4	$y = 0.7360x + 808.94$	0.9952
MY-ARC—1:3	$y = 0.8255x + 527.14$	0.9976	MY-ARC—1:4	$y = 0.7738x + 694.43$	0.9819

3.3. Evolution of the Dynamic Young's Modulus and Its Relation to the Physical Properties of the Processed Mortars

Firstly, Table 7 presents some of the most relevant physical properties of cement mortars that were measured at the age of 28 days, as indicated by the UNE-EN 196-1 standard [53].

Table 7. Physical properties of mortars made with recycled aggregate after 28 days.

Property	Adherence (N/mm ²)		Hardness (Shore D)		Absorption (kg/mm ² min ^{0.5})		Real Density (kg/m ³)	
	1:3	1:4	1:3	1:4	1:3	1:4	1:3	1:4
Mortar								
MY-NA	0.53	0.49	81	77	0.53	0.55	2439	2286
MY-ARH	0.41	0.37	74	72	0.61	0.67	2322	2270
MY-ARC	0.42	0.39	73	70	0.65	0.69	2231	2197

Analyzing Table 7, we can see that the adherence represented by the ability of the mortars to absorb normal stresses to the application surface is higher in mortars made with natural aggregate. This is due to the higher fineness content and impurities of aggregates from CDW, which decrease their adherence. Furthermore, it can be seen that the higher the cement content in the mix, the higher the adhesion values [56]. In all cases, the resistance to adhesion was higher than the 0.30 N/mm² required by the UNE-EN 998-1: 2018 standard [57].

The surface hardness measured in Shore D units was also reduced in mortars made from the recycled aggregate. Furthermore, in Table 7, it can be seen that the absorption of water by capillarity, which depends directly on the porosity of the material, was higher in mortars made with recycled aggregate, especially in those dosages with a cement/aggregate ratio of 1:4. This higher absorption rate can cause problems if this type of material is placed outdoors and exposed to frequent rainfall, as in the case of efflorescence or humidity. In any case, the mortars made with recycled ceramic aggregate had higher absorption values. Finally, it was verified that a greater compactness with a cement/aggregate ratio of 1:3 favored higher real-density values. As in the other properties, mortars made with natural aggregate had higher frequencies than their counterparts made with recycled aggregates.

Figures 9 and 10 show the results derived from the evolution of the dynamic Young's modulus and its relationship with the most relevant mechanical properties of masonry mortars—flexural strength and compression. For this, tests were carried out on test tubes from the same mix at ages 7, 14, 28, 56 and 72 days for each of the dosages studied and in a laboratory environment (cured in a humid chamber at 20 °C and 80% relative humidity).

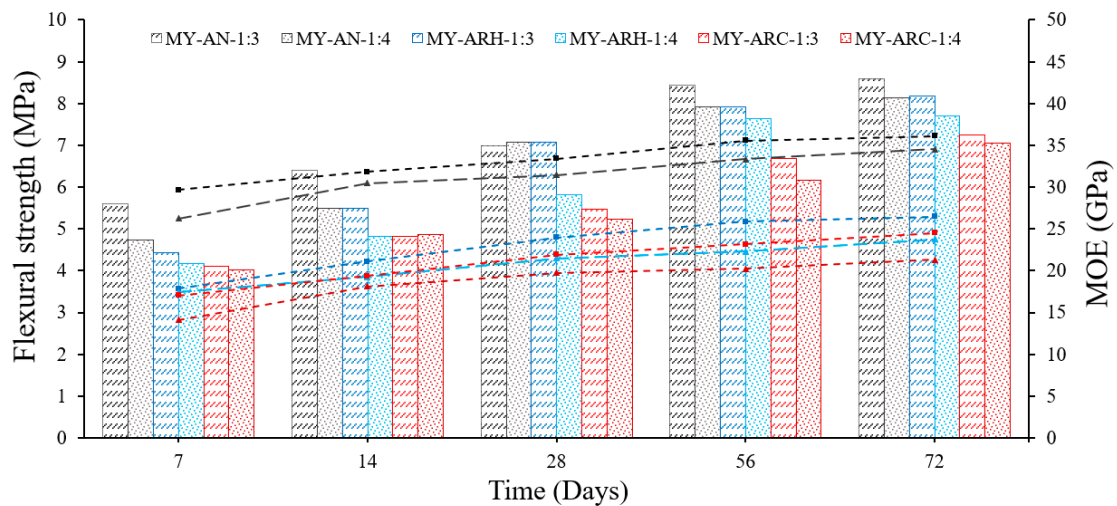


Figure 9. The evolution of the flexural strength (bars) and dynamic Young’s Modulus (dotted lines) measured over time for the different dosages used.

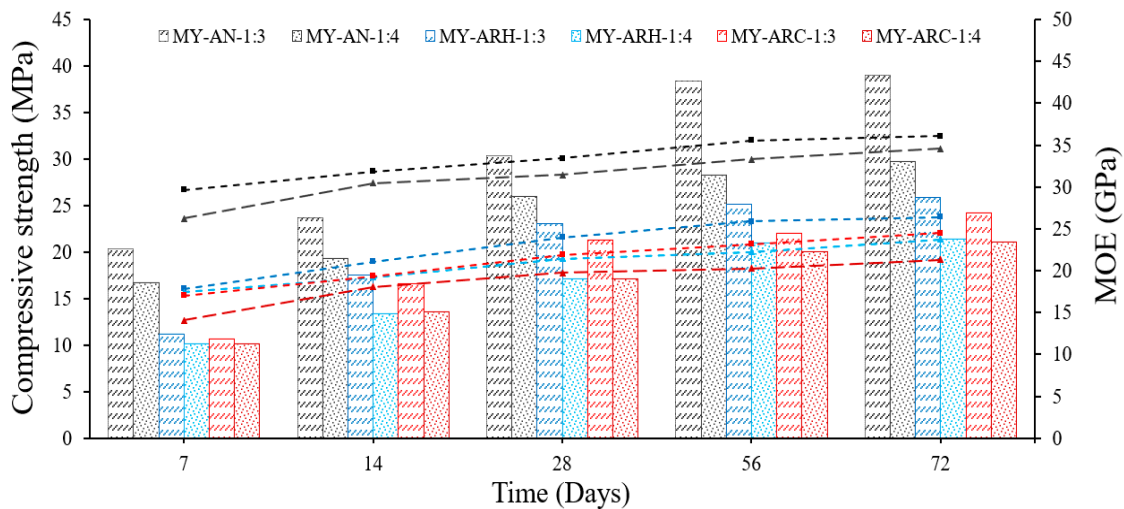


Figure 10. The evolution of the compressive strength (bars) and dynamic Young’s modulus (dotted lines) measured over time for the different dosages used.

As is known, mortar acts as a resistant connection element in most applications. It is capable of transmitting the stresses of the construction system of which it is a part and distributing the loads acting on it. In the analysis of Figures 9 and 10, an increase in the mechanical resistance of flexion and compression is observed as the time since mixing increases. In this sense, a rapid growth of resistance at an early age is observed, which stabilizes after 56 days. In the same graphs, the progress of the dynamic Young’s modulus has been represented with a dashed line, indicating the values obtained at the suggested ages. Regarding mechanical properties, the better performance of mortars made with natural aggregate can be seen, with mortars made with recycled ceramic aggregate having the lowest strength. Besides, as was the case with other physical properties presented in Table 7, the highest dosages in cement with a 1:3 ratio showed higher flexural and compressive strength values than their counterparts with a cement/aggregate ratio of 1:4. Regarding the compressive strength, in all the mixes tested, the minimum resistant classification M of 7.5 MPa for mortars with application in plasters and plasters established by the UNE-EN 998-1: 2018 standard [57] was exceeded. Furthermore, following other studies exploring how the dynamic Young’s modulus evolves rapidly at an early age and later

begins to stabilize, the variations produced in this property were proportional to those observed in the evolution of static mechanical resistance [58].

The results derived from the shrinkage test carried out on specimens with a size of $25 \times 25 \times 287 \text{ mm}^3$ following the recommendations of the UNE 80-112-89 standard are shown in Figures 11 and 12. This test is particularly relevant in mortars made with recycled aggregate, where this typology of materials is sometimes not capable of withstanding the stresses produced by the rapid evaporation of water, giving rise to cracks and imperfections during curing [59].

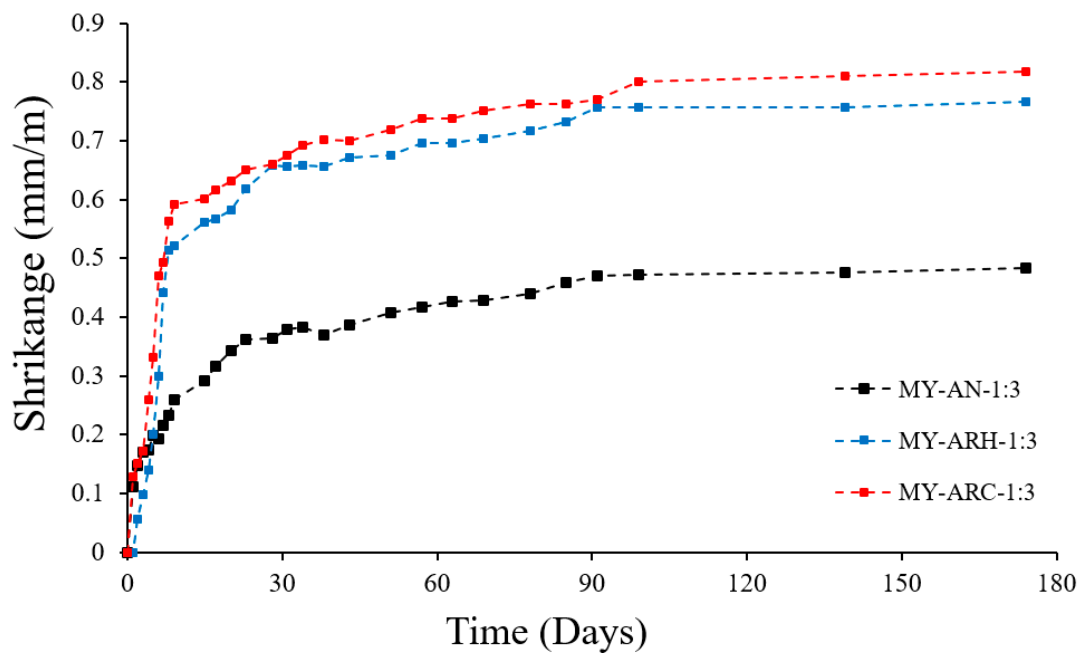


Figure 11. Evolution of shrinkage (mm/m) versus time (days). Cement mortars with a cement/aggregate ratio of 1:3.

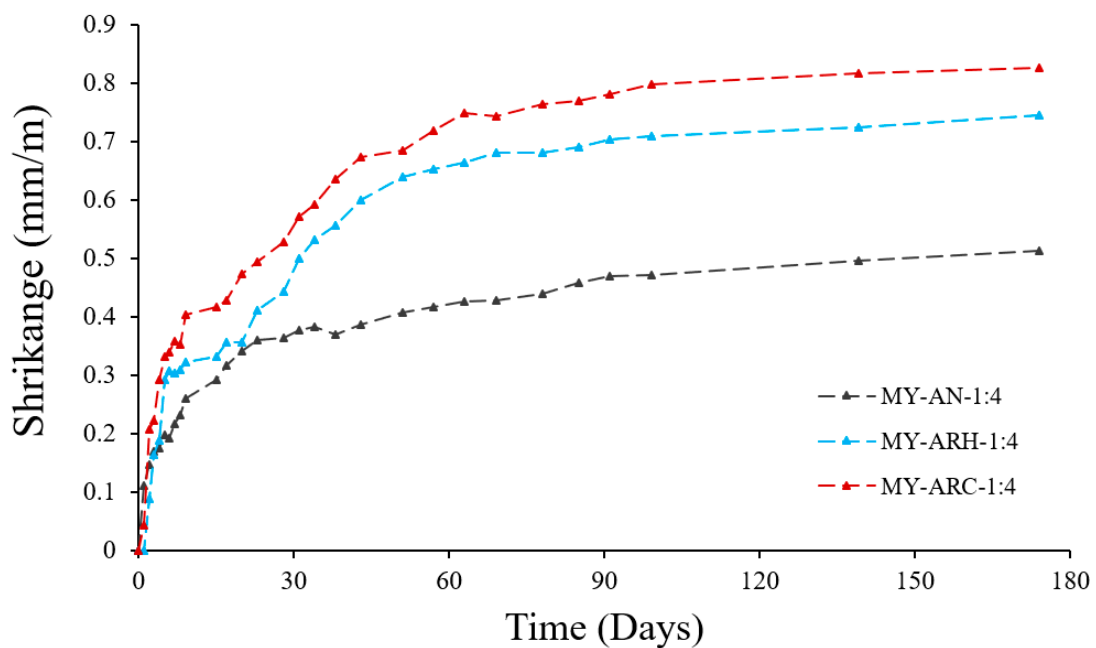


Figure 12. Evolution of shrinkage (mm/m) versus time (days). Cement mortars with a cement/aggregate ratio of 1:4.

As can be seen in Figures 11 and 12, following the greater absorption of recycled aggregates shown in Table 3, the values of shrinkage during setting were higher in mortars made with aggregates from CDW than in those made with natural aggregate. The specimens of recycled ceramic aggregate presented higher shrinkage values than those made with aggregates from concrete waste. These values agree with those obtained in previous investigations and show the negative influence of the content of fine material and residues adhered to the recycled aggregates [60].

Finally, in Figure 13, as an example of the correct setting of the mixes made with recycled aggregate, the images collected with the help of a scanning electron microscope (SEM) are reflected for the blend made with recycled concrete aggregate and cement/aggregate at a ratio of 1:3 at 28 days. This test was carried out using a JEOL JSM-820 scanning electron microscope, applying a gold surface coating to the dried samples to improve electronic conduction. The software used by the equipment for the acquisition, treatment and evaluation of the analysis was the EDX Oxford ISIS-Link ©.

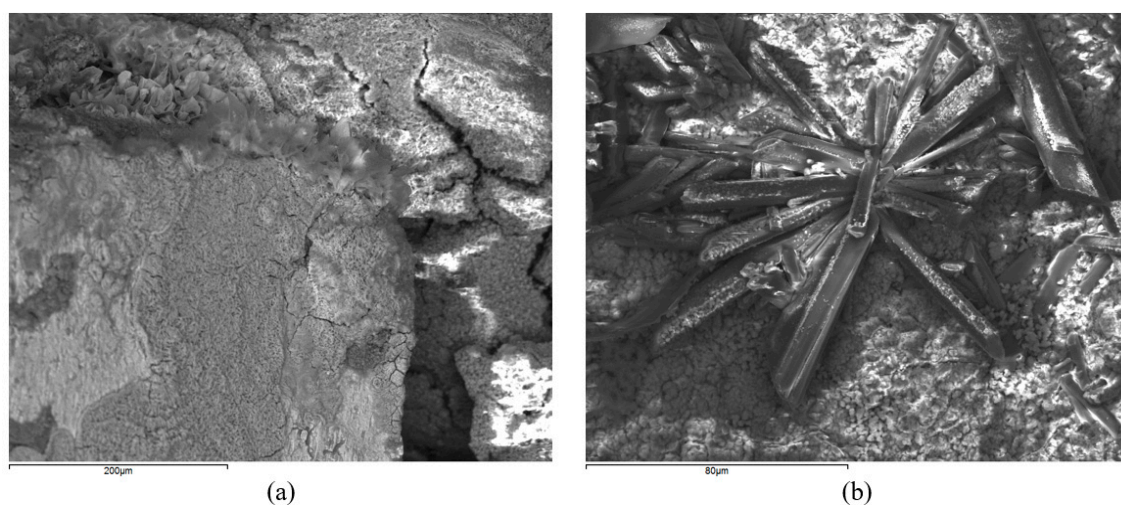


Figure 13. Microscopies performed on the cement mortar sample made with recycled concrete aggregate and cement/aggregate at a ratio of 1:3 at the age of 28 days: (a) Mortar matrix; (b) Ettringite crystal.

The type of test shown in Figure 13 allows the textural, morphological and chemical characterizations of the mortar samples to be determined. The analysis was carried out on one of the two fractured parts that separated after carrying out the flexural strength test. Figure 13a shows the uniformity in the distribution of the mortar matrix as well as the good compactness and adherence of the binder to the aggregate. This good compactness is related to the increase in density, which increases the ease of transmitting the ultrasound waves through the mortar and allows higher values of the dynamic Young's modulus to be obtained. Finally, in Figure 13b, we present the formation of ettringite crystals in the hardened mortar at the age of 28 days. A chemical compound of high relevance in this type of material is generated from the reaction of tricalcium aluminates with calcium sulfate [61]. These results are complementary to other studies carried out by various authors on cement pastes with additives, where it has been shown that the dynamic modulus of elasticity of pastes increased when the water–cement ratio decreased [62].

4. Conclusions

A simple and efficient method has been developed to determine the dynamic Young's modulus through the measurement of the vibrations induced on the surface of the finished mortar specimens. The Arduino low-cost accelerometer sensor used in this work reliably collected the propagation velocity values of mechanical disturbances through the designed mortars. The correlation between the results obtained by the traditional method based on the emission and capture of ultrasonic waves and the alternative method designed with Arduino accelerometers has been established, observing

a strong positive linear relationship. The fact that this correlation is present allows us to consider future applications of this measurement technique, designed for the determination of dynamic Young's modulus at the laboratory level, in industries involved in the production of cement mortars who may wish to use this system as a tool for quality control.

Our approach allows us to more deeply understand the characterization of mortars, and it has been verified that mortars made with aggregates from CDW obtain lower values of their dynamic Young's modulus, which translates into a lower flexural strength than mortars made with natural aggregate. Of the two aggregates studied in this work, the recycled aggregate from ceramic waste had the worst properties for the production of cement mortars. The cement/aggregate ratio is also decisive in terms of the final properties of cement/aggregate, with the ratio of 1:4 having the lowest deformation capacity regardless of the nature of the aggregate used. In this way, the results reflect that dosage with a cement/aggregate ratio of 1:3 by weight would be optimal for use in the preparation of masonry mortars.

The study of the evolution of mechanical properties over time has shown that resistance to flexion and compression increases rapidly at the beginning of the process and tends to stabilize its value after nearly 56 days. Besides this, in all cases, it was found that mortars made with natural aggregate had higher strengths; additionally, mortars that were more abundant in cement (with a 1:3 ratio) showed better results. The progression in these resistances is related to the evolution of the dynamic Young's modulus, as measured in all the mixes. Besides this, the compressive strength results showed that it is possible to use this type of mortar—made with recycled aggregate—for the production of masonry mortars to be used in the execution of brick facades.

In addition, it was also possible to determine the lower density of recycled aggregates and their higher absorption coefficients, especially in recycled ceramic aggregate. The greater adherence of mortars made with natural aggregate, which have less fineness, which increases in cement/aggregate ratios of 1:3 compared to 1:4, was also shown. In the shrinkage test, it was possible to verify that the stability of the volume during setting was higher in the mixes made with natural aggregate than with mortars made with recycled ceramic aggregate, presenting higher shrinkage values regardless of the cement/aggregate ratio.

Author Contributions: Conceptualization, D.F. and C.M.; methodology, D.F.; software, E.Y. and E.G.; validation, D.F., E.Y. and E.G.; formal analysis, D.F. and C.M.; investigation, E.G. and E.Y.; resources, C.M.; data curation, E.Y.; writing—original draft preparation, D.F. and E.Y.; writing—review and editing, E.Y.; visualization, D.F.; supervision, C.M.; funding acquisition, C.M. All authors have read and agreed to the published version of the manuscript.

Funding: This research was funded by Universidad Politécnica de Madrid.

Acknowledgments: The authors want to express their gratitude to all the companies and laboratories that have collaborated and provided their facilities to carry out this work.

Conflicts of Interest: The authors declare no conflict of interest.

References

1. Vidales, A. Caracterización Físicoquímica y Aplicaciones de Yeso con Adición de Residuo Plástico de Cables Mediante Criterios de Economía Circular. Ph.D. Thesis, E.T.S. de Edificación, Universidad Politécnica de Madrid, Madrid, Spain, 2019. [[CrossRef](#)]
2. Siddiqi, A.; Haraguchi, M.; Narayanamurti, V. Urban waste to energy recovery assessment simulations for developing countries. *World Dev.* **2019**, *131*. [[CrossRef](#)]
3. Piña, C.; Del Rio, M.; Viñas, C.; Vidales, A.; Kosior, M. Analysis of the mechanical behaviour of the cement mortars with additives of mineral wool fibres from recycling of CDW. *Constr. Build. Mater.* **2019**, *210*, 56–62. [[CrossRef](#)]
4. Lam, P.; Yu, A.; Wu, Z.; Su Poon, C. Methodology for upstream estimation of construction waste for new building projects. *J. Clean. Prod.* **2019**, *230*, 1003–1012. [[CrossRef](#)]

5. Pacheco-Torgal, F.; Ding, Y.; Colangelo, F.; Tuladhar, R.; Koutamanis, A. *Advances in Construction and Demolition Waste Recycling: Management, Processing and Environmental Assessment*; Woodhead Publishing: Cambridge, UK, 2020.
6. Silva, R.V.; De Brito, J.; Dhir, R.K. Use of recycled aggregates arising from construction and demolition waste in new construction applications. *J. Clean. Prod.* **2019**, *236*, 117629. [[CrossRef](#)]
7. Mistri, A.; Kumar, S.; Dhami, N.; Mukherjee, A.; Barai, S.V. A review on different treatment methods for enhancing the properties of recycled aggregates for sustainable construction materials. *Constr. Build. Mater.* **2020**, *233*, 117894. [[CrossRef](#)]
8. Kox, S.; Vanroelen, G.; Van Herck, J.; De Krem, H.; Vandorem, B. Experimental evaluation of the high-grade properties of recycled concrete aggregates and their application in concrete road pavement construction. *Case Stud. Constr. Mater.* **2020**, *11*. [[CrossRef](#)]
9. Etxeberria, M.; Vázquez, E.; Marí, A.; Barra, M. Influence of amount of recycled coarse aggregates and production process on properties of recycled aggregate concrete. *Cem. Concr. Res.* **2007**, *37*, 735–742. [[CrossRef](#)]
10. Juan-Valdés, A.; Rodríguez, D.; Garcíá, J.; Guerra, M.I.; Morán, J.M. Mechanical and microstructural characterization of non-structural precast concrete made with recycled mixed ceramic aggregates from construction and demolition wastes. *J. Clean. Prod.* **2018**, *180*, 482–493. [[CrossRef](#)]
11. Zhou, H.; Liu, U.; Lu, Y.; Dong, P.; Guo, B.; Ding, W.; Xing, F.; Liu, T.; Dong, B. In situ crack propagation monitoring in mortar embedded with cement-based piezoelectric ceramic sensors. *Constr. Build. Mater.* **2016**, *126*, 361–368. [[CrossRef](#)]
12. Gere, J.M. *Timoshenko Resistencia de Materiales*, 5th ed.; Editorial Paraninfo: Madrid, Spain, 2002; ISBN 8497320654.
13. Saiz, P.; Ferrández, D.; Morón, C.; Payán, A. Comparative study of the influence of three types of fibre in the shrinkage of recycled mortar. *Mater. Constr.* **2018**, *68*, 332. [[CrossRef](#)]
14. Jiménez, J.R.; Ayuso, J.; López, M.; Fernández, J.M.; De Brito, J. Use of fine recycled aggregates from a ceramic waste in masonry mortar manufacturing. *Constr. Build. Mater.* **2013**, *40*, 679–690. [[CrossRef](#)]
15. Morón, C.; García, A.; Ferrández, D. Learning process of the vibration generation by impact on floor uses in building engineering students. In Proceedings of the 9th International Technology, Education and Development Conference INTED 2015 (IATED), Madrid, Spain, 2–4 March 2015; pp. 4469–4475, ISBN 978-84-606-5763-7.
16. Carrillo, J.; Ramirez, J.; Lizarazo, J. Modulus of elasticity and Poisson's ratio of fiber-reinforced concrete in Colombia from ultrasonic pulse velocities. *J. Build. Eng.* **2019**, *23*, 18–26. [[CrossRef](#)]
17. Ferrández Vega, Daniel Estudio de la Transmisión de Vibraciones por Impacto en Losas de Hormigón y Mortero. Ph.D. Thesis, E.T.S. de Edificación (UPM), Universidad Politecnica de Madrid, Madrid, Spain, 2016. [[CrossRef](#)]
18. UNE-EN ISO 12680-1:Methods of Test for Refractory Products—Part 1: Determination of Dynamic Young's Modulus (MOE) by Impulse Excitation of Vibration, ISO 12680-1:2005; International Organization for Standardization: Geneva, Switzerland, 2005.
19. Rosell, J.R.; Cantalapiedra, I.R. Simple method of dynamic Young's modulus determination in lime and cement mortars. *Mater. Constr.* **2011**, *61301*, 39–48. [[CrossRef](#)]
20. Bauer, E.; Pavón, E.; Barreira, E.; Kraus, E. Analysis of building facade defects using infrared thermography: Laboratory studies. *J. Build. Eng.* **2016**, *6*, 93–104. [[CrossRef](#)]
21. Guadagnuolo, M.; Aurilio, A.; Basile, A.; Faella, G. Modulus of Elasticity and Compressive Strength of Tuff Masonry: Results of a Wide Set of Flat-Jack Tests. *Buildings* **2020**, *10*, 84. [[CrossRef](#)]
22. Boulay, C.; Staquet, S.; Azenha, M.; Deraemaeker, A.; Crespini, M.; Carette, J.; Granja, J.; Delsaute, B.; Dumoulin, C.; Karaiskos, G. Monitoring elastic properties of concrete since very early age by means of cyclic loadings 2020, ultrasonic measurements, natural resonant frequency of component frequency of composite beam (EMM-ARM) and with smart aggregates. In Proceedings of the VIII International Conference on Fracture Mechanics of Concrete and Concrete Structures (FraMCoS 8), Toledo, Spain, 10–14 March 2013.
23. Lourenço, T.; Matías, L.; Faira, P. Anomalies detection in adhesive wall tiling systems by infrared thermography. *Constr. Build. Mater.* **2017**, *148*, 419–428. [[CrossRef](#)]
24. Mustafa, A.; Mahmoud, M.A.; Abdurhaem, A.; Furquan, S.A.; Al-Nakhli, A.; BaTaweel, M. Comparative Analysis of Static and Dynamic Mechanical Behavior for Dry and Saturated Cement Mortar. *Materials* **2019**, *12*, 3299. [[CrossRef](#)]

25. Yedra, E.; Ferrández, D.; Saiz, P.; Morón, C. Low cost system for measuring the evolution of mechanical properties in cement mortars as a function of mixing water. *Constr. Build. Mater.* **2020**, *244*, 118–127. [[CrossRef](#)]
26. Barroca, N.; Borges, L.M.; Velez, F.J.; Monteiro, F.; Gorski, M.; Castro-Gomes, J. Wireless sensor networks for temperature and humidity monitoring within concrete structures. *Constr. Build. Mater.* **2013**, *40*, 1156–1166. [[CrossRef](#)]
27. Ferrández, D.; Yedra, E.; Morón, C.; Morón, A. Alternative tests for the determination of the setting time. Capacitive and resistive methods. *DYNA* **2020**, *953*, 294–298. [[CrossRef](#)]
28. Craveiro, F.; Nazarian, S.; Bartolo, P.J.; Pinto, J. An automated system for 3D printing functionally graded concrete-based materials. *Addit. Manuf.* **2020**, *33*. [[CrossRef](#)]
29. Panda, B.; Hui, J.; Jen, M. Mechanical properties and deformation behaviour of early age concrete in the context of digital construction. *Compos. Part B Eng.* **2019**, *165*, 563–571. [[CrossRef](#)]
30. Ausweger, M.; Binder, E.; Lahayne, O.; Reihnsner, R.; Maier, G.; Peyerl, M.; Pichler, B. Early-Age Evolution of Strength, Stiffness, and Non-Aging Creep of Concretes: Experimental Characterization and Correlation Analysis. *Materials* **2019**, *12*, 207. [[CrossRef](#)] [[PubMed](#)]
31. Morón, C.; Diaz, J.P.; Ferrández, D.; Ramos, M.P. Mechatronic Prototype of Parabolic Solar Tracker. *Sensors* **2016**, *16*, 882. [[CrossRef](#)]
32. Morón, C.; Ferrández, D.; Saiz, P.; Morón, A. Automatic System for Detection and Positioning of Impacts in Metals Based on Arduino. *Shock Vib.* **2019**, *2019*, 9675898. [[CrossRef](#)]
33. García Meseguer, A.; Morán Cabré, F.; Arroyo Portero, J.C. *Jiménez Montoya: Hormigón Armado*, 15th ed.; Editorial Gustavo Gili: Barcelona, Spain, 2011.
34. Wolfs, R.J.M.; Bos, F.P.; Salet, T.A.M. Early age mechanical behaviour of 3D printed concrete: Numerical modelling and experimental testing. *Cem. Concr. Res.* **2018**, *106*, 103–116. [[CrossRef](#)]
35. Gil, L.; Bernat, E.; Cañavate, J. Changes in Properties of Cement and Lime Mortars When Incorporating Fibers from End-of-Life Tires. *Fibers* **2016**, *4*, 7. [[CrossRef](#)]
36. *Methods of Test for Mortar for Masonry—Part 11: Determination of Flexural and Compressive Strength of Hardened Mortar*; UNE-EN 1015-11:2000/A1; European Committee for Standardization: Brussels, Belgium, 2000.
37. *Methods of Test for Mortar for Masonry—Part 12: Determination of Adhesive Strength of Hardened Rendering and Plastering Mortars on Substrates*; UNE-EN 1015-12:2016; European Committee for Standardization: Brussels, Belgium, 2016.
38. *Methods of Test for Mortar for Masonry—Part 18: Determination of Water Absorption Coefficient due to Capillary Action of Hardened Mortar*; UNE-EN 1015-18:2003; European Committee for Standardization: Brussels, Belgium, 2003.
39. *Métodos de Ensayo de Cementos: Ensayos Físicos: Determinación de la Retracción de Secado y del Hinchamiento en Agua*; UNE 80-112-89; AENOR: Madrid, Spain, 1989.
40. Spanish Ministry of Public Works. *Instrucción de Hormigón Estructural EHE-08 (Spanish Structural Concrete Code)*; BOE: Madrid, Spain, 2008; Volume 203, p. 258e66.
41. Cement Permanent Commission. *Instruction for the Receipt of Cement*; RC-08; Ministry of Public Works and Transport: Madrid, Spain, 2009.
42. Piña, C.; Atanes Sánchez, E.; Del Río, M.; Viñas, C.; Vidales, A. Feasibility of the use of mineral wool fibres recovered from CDW for the reinforcement of conglomerates by study of their porosity. *Constr. Build. Mater.* **2018**, *191*, 460–468. [[CrossRef](#)]
43. *Aggregates for Mortar*; UNE-EN 13139:2002; European Committee for Standardization: Brussels, Belgium, 2002.
44. *Tests for Geometrical Properties of Aggregates—Part 1: Determination of Particle Size Distribution—Sieving Method*; UNE-EN 933-1:2012; European Committee for Standardization: Brussels, Belgium, 2012.
45. *Aggregates for Concrete: Determination of the Coefficient of Friability of the Sands*; UNE-EN 146404:2018; European Committee for Standardization: Brussels, Belgium, 2018.
46. *Tests for Mechanical and Physical Properties of Aggregates—Part 3: Determination of Loose Bulk Density and Voids*; UNE-EN 1097-3:1999; European Committee for Standardization: Brussels, Belgium, 1999.
47. *Tests for Mechanical and Physical Properties of Aggregates—Part 6: Determination of Particle Density and Water Absorption*; UNE-EN 1097-6:2014; European Committee for Standardization: Brussels, Belgium, 2014.

48. *Test for Geometrical Properties of Aggregates: Part 2: Determination of Particle Size Distribution: Test Sieves 2003, Nominal Size of Apertures*; UNE-EN 933-2:1996; European Committee for Standardization: Brussels, Belgium, 1996.
49. *Norma Básica de Edificación: Muros Resistentes de Fábrica de Ladrillo*; NBE FL-90; Ministerio de Obras Públicas y Urbanismo: Madrid, Spain, 1990.
50. Ulsen, C.; Kahn, H.; Hawlitscschek, G.; Masini, E.A.; Angulo, S.C.; John, V.M. Production of recycled sand from construction and demolition waste. *Constr. Build. Mater.* **2013**, *40*, 1168–1173. [[CrossRef](#)]
51. Saiz, P.; Ferrández, D.; Morón, C.; Fernández, F. Behaviour of masonry mortars fabricated with recycled aggregate towards moisture. *DYNA* **2019**, *94*, 442–446. [[CrossRef](#)]
52. Bustos García, A. *Morteros con Propiedades Mejoradas de Ductilidad por Adición de Fibras de Vidrio, Carbono y Basalto*. Ph.D. Thesis, E.T.S. de Edificación. Universidad Politécnica de Madrid, Madrid, Spain, 2018.
53. *Methods of Testing Cement—Part 1: Determination of Strength*; UNE-EN 196-1:2018; European Committee for Standardization: Brussels, Belgium, 2018.
54. *Methods of Test for Mortar for Masonry—Part 2: Bulk Sampling of Mortars and Preparation of Test Mortars*; UNE-EN 1015-2:1999/A1:2007; European Committee for Standardization: Brussels, Belgium, 2007.
55. Vidya, R.; Raghu, B.K.; Shantha, S. An experimental study on cracking evolution in concrete and cement mortar by the b-value analysis of acoustic emission technique. *Cem. Concr. Res.* **2012**, *428*, 1094–1104. [[CrossRef](#)]
56. Kumar, G. Influence of fluidity on mechanical and permeation performances of recycled aggregate mortar. *Constr. Build. Mater.* **2019**, *213*, 404–412. [[CrossRef](#)]
57. *Specification for Mortar for Masonry—Part 1: Rendering and Plastering Mortar*; UNE-EN 998-1:2016; European Committee for Standardization: Brussels, Belgium, 2016.
58. Deniz, S.; Erdoğan, S. Prediction of Elastic Moduli Development of Cement Mortars Using Early Age Measurements. *J. Mater. Civil. Eng.* **2015**, *27*. [[CrossRef](#)]
59. Garbalińska, H.; Wygocka, A. Microstructure modification of cement mortars: Effect on capillarity and frost-resistance. *Constr. Build. Mater.* **2014**, *51*, 258–266. [[CrossRef](#)]
60. Gorospe, K.; Booya, E.; Ghaednia, H.; Das, S. Effect of various glass aggregates on the shrinkage and expansion of cement mortar. *Constr. Build. Mater.* **2019**, *210*, 301–311. [[CrossRef](#)]
61. Tian, X.; Zhou, Z.; Xin, Y.; Jiang, L.; Zhao, X.; An, Y. A novel sulfate removal process by ettringite precipitation with aluminum recovery: Kinetics and a pilot-scale study. *J. Hazard. Mater.* **2019**, *365*, 572–580. [[CrossRef](#)]
62. Zhao, H.; Huang, D.; Wang, X.; Chen, X. Dynamic elastic modulus of cement paste at early age based on nondestructive test and multiscale prediction model. *J. Wuhan Univ. Technol. Mat. Sci.* **2014**, *29*, 321–328. [[CrossRef](#)]

Publisher’s Note: MDPI stays neutral with regard to jurisdictional claims in published maps and institutional affiliations.



© 2020 by the authors. Licensee MDPI, Basel, Switzerland. This article is an open access article distributed under the terms and conditions of the Creative Commons Attribution (CC BY) license (<http://creativecommons.org/licenses/by/4.0/>).